A Fourth-Order, Density-Functional, Random-Phase Approximation Study of Monomer Segregation in Phase-Separated, Lamellar, Diblock-Copolymer Melts

William E. McMullen

Department of Chemistry, Texas A&M University, College Station, Texas 77843-3255

Received July 27, 1992; Revised Manuscript Received October 6, 1992

ABSTRACT: We show that the random-phase approximation (RPA) for correlations in block-copolymer melts derives from the free energy functional of ideal chains augmented by a random-mixing approximation for the interactions between monomers. The derivation facilitates comparisons to other approaches to monomer segregation. We apply the RPA functional to the segregation of symmetric, lamellar, block-copolymer phases while employing the full wave-vector dependence of the third- and fourth-order vertex functions. Compared to calculations which accurately treat only the second-order vertex function, the fourth-order theory shows that the wave-vector dependence of the higher-order terms plays an important role in determining the degree of segregation of the melt. The approach to the strong-segregation limit (SSL) is very slow, so the scaling of the domain size D with the polymerization number N obeys the predicted relation $D \propto N^{2/3}$ only for very long chains and low temperatures. In contrast, the second-order theory approaches the SSL scaling result more rapidly, again underscoring the importance of higher-order vertex functions. In the weak-segregation limit (WSL), the interfacial width rises rapidly, reaching a maximum before decreasing and then relaxing to an almost constant value in the SSL.

I. Introduction

Block-copolymer melts composes of even slightly incompatible sequences of monomers generally undergo a microphase separation[1] at moderate temperatures. The microphase separation differs, however, from the phase separation of other types of liquids in that the regions rich in different types of monomers cannot distance themselves from each other over macroscopic length scales. Instead, the physical connectivity of the different blocks comprising the copolymer chains dictates that segregation occurs over distances comparable to the size of individual blocks. As one of the more interesting consequences of the connectivity of the blocks, microphase separations and the morphologies of the resulting domain structures have been the subject of numerous experimental (e.g., refs 2 and 3 and the review of ref 4) and theoretical[5-15] investigations. A large percentage of the theories of block-copolymer thermodynamics employ vertex-function expansions based on the random-phase approximation (RPA).[6] However, with few exceptions,[9a,14] the vertex-function-based calculations have been limited to weakly segregated morphologies[6,11,12,16] in which the number density of the copolymer species varies sinusoidally. For such degrees of segregation, a single Fourier mode (or single family of Fourier modes) suffices to describe the density profile. The purpose of the present article is to study the effects of higher-order vertex-function contributions to the block-copolymer morphology and to show how the expansion-based theory compares to other approaches to block-copolymer segregation. Others[12,16] have previously examined higher-order contributions in the weak-segregation limit, but the calculations outlined here investigate the role of fourth-order contributions in the strong- and intermediate-segregation cases as well.

For complex morphologies or when the chain architecture involves branching or several different blocks, the density-functional formalism which leads to the RPA vertex-function expansion has important practical advantages over alternative, but formally equivalent self-consistent-field (scf) theories[5,15] of inhomogeneous block-copolymer fluids. The scf theories are based on modified diffusion equations for monomer distribution functions and derive from the Markov properties of random-flight chains in external fields. Segregated block copolymers may have lamellar (one-dimensional), hexagonal (2-D), body-centered cubic (3-D), or ordered bicontinuous double-diamond (3-D) morphology.[4,6] Except in the lamellar case, solving the scf differential equation to obtain the equilibrium state appears difficult if not infeasible. Recently,[15] Shull has employed the scf approach to calculate the equilibrium profile of diblock copolymers in the lamellar state. His results thus represent the exact solution of the approximate functional upon which the scf formalism is based. The approximate density-functional calculations described in the present article represent an approximate solution of the same functional but also possess sufficient flexibility for applications to more complex morphologies and chain architectures. This motivates comparisons of the present, fourth-order vertex-function calculations to the numerically exact scf ones. As discussed below, we find that the scf and approximate density-functional calculations agree qualitatively in every way, though quantitative discrepancies appear at strong degrees of segregation. It seems reasonable, without further information, to expect similar agreement between the unknown, exact solutions of the free energy functional for two- and three-dimensional morphologies and the fourth-order density functional.

The most well-characterized block-copolymer mesophase is the lamellar one in which domains form a one-dimensional pattern of wavelength D. Recent experiments[3,4] show that the boundary region—the interface—between domains may involve substantial mixing of the incompatible monomers. This effect becomes less significant[3,14] at low temperatures when the domains segregate strongly—the so-called strong-segregation limit (SSL). In the weak-segregation limit (WSL), the region in which different monomers mix appreciably becomes as large as the domains themselves, and the notion of an interface ceases to be a useful concept for understanding the microphase separation. Many workers have postulated[6,14] that in the WSL, the domain spacing scales as the square root of the polymerization number N. However, more careful theoretical treatments[12,15,16] suggest that the

0024-9297/93/2226-1027$04.00/0

domain size actually increases more rapidly than $N^{1/2}$ in the WSL. In the SSL, however, simple physical arguments[8,9a,b] support the well-accepted scaling relation $D \propto N^{2/3}$.

The theoretical section following this discussion consists of two parts. In the first section, we rederive the RPA using simple density-functional methods. Some of the ideas employed in our discussion of the RPA also appear in the block-copolymer studies of Semenov[8] and Ohta and Kawasaki[9a] as well as in calculations of the effective χ parameter[17] of polymer blends. However, the precise relation between the RPA vertex-function expansion, density-functional techniques, and the scf formalism remains somewhat vague in these references. Within the context of the present article, it proves useful to provide a brief derivation of the RPA formulation of the problem based entirely on density-functional arguments. This is accomplished by dividing the free energy into two parts: first, an entropic part for the statistics of the chains and second, the usual random-mixing, nonideal energy contribution. This division immediately establishes the connection between the scf, RPA, and density-functional approach to inhomogeneous polymer fluids and leads to a number of current theories of inhomogeneous, homopolymer fluids and blends. Dropping the incompressibility constraint usually invoked with the RPA produces the same set of structure factors derived previously[18,19] using functional integrals. Within the density-functional methodology, the incompressibility condition places a constraint on the allowed density variations and not on the free energy functional itself. Extensions which allow for density fluctuations ignored by the incompressible theory may be obtained from the same functional which leads to the usual, incompressible RPA theory.

After reviewing the RPA in the theoretical section following the Introduction, we employ the fourth-order vertex function to calculate the segregation and domain spacing in symmetric, lamellar, diblock-copolymer melts. For comparison, we repeat the calculations using just the second-order RPA functional supplemented by a heuristic ideal free energy functional. As others have done,[9a,b,12,14-16] we study the growth of the lamellar domain spacing as a function of the temperature (expressed in terms of the Flory parameter χ) and the polymerization number N. We employ the ingenious variational function invented by Melenkevitz and Muthukumar[14] for studying the weak-, intermediate-, and strong-segregation limits of the phase separation. Our numerical calculations differ from those in ref 14 in our use of the full wave-vector dependence of the third- and fourth-order vertex functions. The latter refinements greatly increase the computational burden associated with our studies but also have a moderate quantitative effect on the predictions of the theory. Indeed, we reach the conclusion that while the fourth-order terms approximated by constants in previous calculations[14] contribute only a small fraction of the total free energy, they play an important role in the segregation process. The last section of the main text summarizes the theoretical findings and discusses avenues for theoretical improvement.

II. A Density-Functional Derivation of the Random Phase Approximation Free Energy Functional

The free energy functional

$$F[\{\rho_i(\mathbf{R})\}] = F_G[\{\rho_i(\mathbf{R})\}] + F_{local}[\{\rho_i(\mathbf{R})\}] \quad (1)$$

with $F_G[\{\rho_i(\mathbf{R})\}]$ the free energy functional of inhomogeneous, Gaussian chains and

$$F_{local}[\{\rho_i(\mathbf{R})\}] = \frac{\beta}{2}\sum_{\alpha\beta}\int d1\, u_{\alpha\beta}\rho_\alpha(1)\,\rho_\beta(1) \quad (2)$$

generates the celebrated random-phase approximation (RPA) of polymer melts. The set of densities $\{\rho_i(\mathbf{R})\}$ which appear in eqs 1 and 2 are grand-canonical averages of the monomer number-density operators, $\beta = 1/k_BT$, and we use $\mathbf{R}$ to denote an arbitrary dependence of the set of densities $\{\rho_i(\mathbf{R})\}$ on the spatial coordinates. Ordinary numbers denote integration variables (e.g., $\int d1 = dx_1\, dy_1\, dz_1$). The free energy functional (or, more properly, the *intrinsic* free energy functional[20]) can be written as

$$F[\{\rho_i(\mathbf{R})\}] = \sum_\alpha \int d1\, \rho_\alpha(1)[\ln \rho_\alpha(1)\Lambda_\alpha^3 - 1] - \Phi[\{\rho_i(\mathbf{R})\}] \quad (3)$$

The constants Λ_α appearing in eq 3 have units of length, but their precise definition has no bearing on the analysis that follows.

For atomic systems, $\Phi[\{\rho_i(\mathbf{R})\}]$ contains the nonideal and nonlocal interactions between the particles whose densities appear as its arguments, and functional derivatives of $\Phi[\{\rho_i(\mathbf{R})\}]$ with respect to the densities generate a hierarchy of generalized direct correlation functions.[20] The first part of the right-hand side of eq 3 is the ideal entropy of mixing of the atoms. Functional derivatives of $\Phi[\{\rho_i(\mathbf{R})\}]$ with respect to the monomer number densities also generate the direct correlation functions of monomers in systems of polymers, but the separation of $F[\{\rho_i(\mathbf{R})\}]$ into the two terms on the right-hand side of eq 3 does not provide any practical, computational advantages. For block copolymers, it proves more convenient to focus on the vertex functions defined[6] as

$$\Gamma_{\alpha\beta\ldots\gamma\lambda}(1,2,\ldots,n-1,n) = \frac{\delta^n F[\{\rho_i(\mathbf{R})\}]}{\rho_\alpha(1)\,\rho_\beta(2)\ldots\rho_\gamma(n-1)\,\rho_\lambda(n)} = (-1)^n(n-1)\frac{\delta_{\alpha\beta}\ldots\delta_{\gamma\lambda}}{\rho_\alpha(1)\,\rho_\beta(2)\ldots\rho_\gamma(n-1)\,\rho_\lambda(n)} \times \delta(1-2)\ldots\delta(n-(n-1)) + c_{\alpha\beta\ldots\gamma\lambda}(1,2,\ldots,n-1,n) \quad (4)$$

with the $c_{\alpha\beta\ldots\gamma\lambda}$'s monomer–monomer direct correlation functions and $n \geq 2$. The functional $F[\{\rho_i(\mathbf{R})\}]$ is a Legendre transform of the grand partition function with respect to modified external fields

$$\phi_\alpha(1) = \beta(\mu_\alpha - u_\alpha(1)) \quad (5)$$

with μ_α the chemical potential per monomer[21] of type α and $u_\alpha(1)$ an external field that acts on an α monomer located at position 1. $F[\{\rho_i(\mathbf{R})\}]$ also has the property[13,20]

$$\delta F/\delta\rho_\alpha(1) = \phi_\alpha(1) \quad (6)$$

The discussion in this section applies to ordinary atomic systems, to mixtures of homopolymers, and to block copolymers. [In the case of polymers, the coordinates refer to centers of mass or geometric centers of the monomers.] However, for concreteness and because polymers are our primary interest, we refer to the particles from now on as monomers. For homogeneous melts, the second-order vertex function has the well-known property[6,20,22]

$$\frac{1}{V}\Gamma_{\alpha\beta}(q,-q) = \frac{1}{\rho}S^{-1}_{\alpha\beta}(q) = \frac{\delta_{\alpha\beta}}{\rho_\alpha} - c_{\alpha\beta}(q) \quad (7)$$

with q a Fourier transform variable, V the volume, ρ the overall number density of monomers, and $S^{-1}_{\alpha\beta}$ an element

of the inverse matrix of monomer–monomer structure factors.

Now consider a slightly inhomogeneous polymer melt. For small overall density variations, it suffices to expand $F[\{\rho_i(\mathbf{R})\}]$ about a homogeneous state $F[\{\rho_i^0\}]$ as

$$F[\{\rho_i(\mathbf{R})\}] = F[\{\rho_i^0\}] + \sum_\alpha \beta\mu_\alpha \int d1\, [\rho_\alpha(1) - \rho_\alpha^0] + \frac{1}{2}\sum_{\alpha\beta}\int d1 \int d2\, \Gamma_{\alpha\beta}(1\text{–}2)[\rho_\alpha(1) - \rho_\alpha^0][\rho_\beta(2) - \rho_\beta^0] + O((\rho_i(\mathbf{R}) - \rho_i^0)^3) \quad (8)$$

In the case of a binary incompressible melt,

$$\rho = \rho_A^0 + \rho_B^0 = \rho_A(1) + \rho_B(1) \quad (9)$$

and

$$\rho_A(1) - \rho_A^0 = -[\rho_B(1) - \rho_\beta^0] \quad (10)$$

Substituting eq 10 into the third term on the right-hand side of eq 8, we find

$$\Gamma_2(1\text{–}2)[\rho_A(1) - \rho_A^0][\rho_A(2) - \rho_A^0] = \sum_{\alpha\beta}\Gamma_{\alpha\beta}(1\text{–}2)[\rho_\alpha(1) - \rho_\alpha^0][\rho_\beta(2) - \rho_\beta^0] = [\rho_A(1) - \rho_A^0][\rho_A(2) - \rho_A^0]\sum_{\alpha\beta}(-1)^{\delta_{\alpha B}+\delta_{\beta B}}\Gamma_{\alpha\beta}(1\text{–}2) \quad (11)$$

Equation 11 defines Γ_2.

Consider next a melt of ideal polymer chains containing two monomeric species (e.g., a binary block copolymer or a binary blend of different homopolymers). In this case, the second-order vertex functions appearing in eq 8 are just the Gaussian inverse structure factors $S^G{}_{\alpha\beta}{}^{-1}(q)$. Then we interpret F as the intrinsic free energy functional of a system of Gaussian chains in a weakly varying external field. Adding to this result the local contribution defined by eq 2, we arrive at the RPA structure factor. To see this, functionally differentiate the sum of eqs 2 and 8 twice with respect to the monomer densities and substitute the result into eq 11. The incompressibility constraint makes a quasi-one-component system out of the binary one and leads to a single unique structure factor $S(q)$ defined as the Fourier transform of $[\rho_A(\mathbf{R}) - \rho_A^0]^2$ (or, due to the incompressibility condition, $[\rho_B(\mathbf{R}) - \rho_B^0]^2$) in the expansion of $F[\rho_A(\mathbf{R}),\rho_B(\mathbf{R})]]$ about $F[\rho_A^0,\rho_B^0]$. Thus,

$$S^{-1}(q) = \frac{\rho\Gamma_2(q,-q)}{V} = S^G{}_{AA}{}^{-1}(q) + S^G{}_{BB}{}^{-1}(q) - 2S^G{}_{AB}{}^{-1}(q) - 2\chi \quad (12)$$

where we have introduced the Flory parameter[23,24]

$$\chi = \frac{\beta}{2}(2u_{AB} - u_{AA} - u_{BB}) \quad (13)$$

A little matrix algebra then leads to

$$S(q) = D(q)/[W(q) - 2\chi D(q)] \quad (14)$$

with

$$W(q) = S_{AA}^G(q) + S_{BB}^G(q) + 2S_{AB}^G(q) \quad (15)$$

and

$$D(q) = \det S^G(q) = S_{AA}^G(q)S_{BB}^G(q) - S_{AB}^G(q)^2 \quad (16)$$

Equation 14 is the standard RPA[6,23] for a binary, incompressible system. However, in deriving this result, we have avoided the use of functional integrals[18,19] or Leibler's response-function[25] algebra—techniques which tend to obscure the underlying simplicity of the RPA as derived from eq 1.

The same procedure applied to the compressible case yields a set of three unique structure factors. Applying eq 4 with $n = 2$ to the sum of eqs 11 (for Gaussian chains) and 2 and solving for the structure factors, we find

$$S_{AA}(q) = \frac{D(q)u_{BB} + S_{AA}^G(q)}{R(q)} \quad (17a)$$

and

$$S_{AB}(q) = \frac{S_{AB}^G(q) - u_{AB}D(q)}{R(q)} \quad (17b)$$

where

$$R(q) = 1 + u_{AA}S_{AA}^G(q) + u_{BB}S_{BB}^G(q) + 2u_{AB}S_{AB}^G(q) + (u_{AA}u_{BB} - u_{AB}^2)D(q) \quad (18)$$

Apart from minor changes in notation, eqs 17 and 18 are identical to the compressible RPA results derived in ref 19 and, in a somewhat different context, also in ref 18. The compressible RPA structure factor $S_{BB}(q)$ follows from eq 17a upon exchanging the A and B subscripts. Equations 17 and 18 differ from the usual RPA (eq 14) in that they allow for arbitrary density fluctuations.

It seems appropriate here to comment briefly about the application of the compressible RPA results to inhomogeneous polymer systems. Researchers have occasionally insinuated that the $q = 0$ divergence of the two-body vertex function Γ_2 results from the incompressibility assumption. Actually, the present derivation shows that the divergence arises from the fixed stoichiometry of the chains rather than the incompressibility condition. In the case of an ideal blend with mole fractions of A and B monomers x_A and x_B for instance, $D(q=0) = x_Ax_BN_AN_B$ because $S_{AA}(0) = x_AN_A$, $S_{BB}(0) = x_BN_B$, and monomers on different chains do not interact so $S_{AB}(0) = 0$. However, $D(q=0)$ in eqs 14 and 17 vanishes for ideal *block*-copolymer chains since $S_{AB}(0) = N_AN_B/N$, ostensibly making the free energy functional in eq 8 undefined (the results of integrating the $\Gamma_{\alpha\beta}(1\text{–}2)$'s over 1 or 2 is undefined) if ρ changes even for *compressible* Gaussian chains. This has nothing to do with the compressibility or assumed lack of compressibility of the chains. In fact, the compressibility κ of a homogeneous fluid of noninteracting block-copolymer chains is given by the ideal-gas-law expression $\kappa = N/\rho k_BT$ which results from the center-of-mass, translational degrees of freedom of each chain.

One can still use eq 8 to describe block copolymers variationally by paying careful attention to the effects of such divergences on the free energy. In particular, the spatially averaged number densities of A and B monomers must reflect the stoichiometry of the chains. Otherwise, the free energy diverges. Alternatively, it may prove helpful, in certain situations, to divide the correlation functions into constant and spatially varying pieces which couple, respectively, to the constant and the spatially varying parts of the densities. Reference 13 contains a detailed account of this methodology. The results of the present article are limited to the incompressible case in order to compare the results of a finite-order, density-functional calculation to other methods. We expect the Gaussian vertex functions derived above to provide a good description of a compressible block-copolymer fluid only if a term is added to F_{local} which explicitly accounts for the fluid's reduced compressibility.

To study block-copolymer microphase separation, we require the third- and fourth-order functional derivatives of $F[\{\rho_i(\mathbf{R})\}]$. Leibler[6] has obtained these as the response functions of a homogeneous system, subject to the incompressibility constraint, to a weak external field. We summarize the salient features of the derivation of these from eq 1. First, note that eq 1 predicts that the third- and higher-order vertex functions do not depend on χ because the local contribution (eq 2) to $F[\{\rho_i(\mathbf{R})\}]$ contains only quadratic and bilinear combinations of the densities. Thus, functional derivatives of $F[\{\rho_i(\mathbf{R})\}]$ higher than second order are independent of the interaction parameters $\{u_{\alpha\beta}\}$. A higher-order theory which allows for monomer–monomer correlations in the interaction part of eq 1 may not lead to such a simplification.

Employing Leibler's[6] notation, define

$$\Gamma_{\alpha\beta\gamma\lambda} = \frac{\delta^4 F}{\delta\rho_\alpha(1)\,\rho_\beta(2)\,\rho_\gamma(3)\,\rho_\lambda(4)} \tag{19}$$

and

$$\Gamma_{\alpha\beta\gamma} = \frac{\delta^3 F}{\delta\rho_\alpha(1)\,\rho_\beta(2)\,\rho_\gamma(3)} \tag{20}$$

Upon expanding $F[\{\rho_i(\mathbf{R})\}]$ (as in eq 8) to fourth order in the density differences and employing the incompressibility constraint (eq 9), we are led naturally to consider the quantities

$$\Gamma_3(1,2,3) = \sum_{\alpha\beta\gamma}(-1)^{\delta_{\alpha B}+\delta_{\beta B}+\delta_{\gamma B}}\Gamma_{\alpha\beta\gamma}(1,2,3) \tag{21}$$

and

$$\Gamma_4(1,2,3,4) = \sum_{\alpha\beta\gamma\lambda}(-1)^{\delta_{\alpha B}+\delta_{\beta B}+\delta_{\gamma B}+\delta_{\lambda B}}\Gamma_{\alpha\beta\gamma\lambda}(1,2,3,4) \tag{22}$$

Using the functional derivative chain rule, one can show[20,21,26]

$$\Gamma_{\alpha\beta\gamma}(1,2,3) = -\int d4\int d5\int d6\;\Gamma_{\alpha s}(1,4)\;\Gamma_{\beta t}(2,5)\;\Gamma_{\gamma v}(3,6)\;G_{stv}(4,5,6) \tag{23}$$

and

$$\begin{aligned}\Gamma_{\alpha\beta\gamma\lambda}(1,2,3,4) = &-\int d5\int d6\int d7\,[\Gamma_{\alpha s\lambda}(1,5,4)\;\Gamma_{\beta t}(2,6)\;\Gamma_{\gamma v}(3,7) + \\ &\Gamma_{\alpha s}(1,5)\;\Gamma_{\beta t\lambda}(2,6,4)\;\Gamma_{\gamma v} + \\ &\Gamma_{\alpha s}(1,5)\;\Gamma_{\beta t}(2,6)\;\Gamma_{\gamma v\lambda}(3,7,4)]G_{stv}(5,6,7) - \\ &\int d5\int d6\int d7\int d8\;\Gamma_{\alpha s}(1,5)\;\Gamma_{\beta t}(2,6)\;\Gamma_{\gamma v}(3,7)\times \\ &\Gamma_{\lambda w}(4,8)\;G_{stvw}(5,6,7,8)\end{aligned} \tag{24}$$

To simplify the notation, we sum over repeated indices in eqs 23 and 24 rather than explicitly indicating summation symbols. The quantities $G_{stv}(5,6,7)$ and $G_{stvw}(5,6,7,8)$ are the three- and four-body density correlation functions

$$G_{stv}(5,6,7) = \langle\Delta\hat{\rho}_s(5)\;\Delta\hat{\rho}_t(6)\;\Delta\hat{\rho}_v(7)\rangle \tag{25}$$

$$G_{stvw}(5,6,7,8) = \langle\Delta\hat{\rho}_s(5)\;\Delta\hat{\rho}_t(6)\;\Delta\hat{\rho}_v(7)\;\Delta\hat{\rho}_w(8)\rangle \tag{26}$$

and the density difference operators $\Delta\hat{\rho}_\alpha(1)$ are defined in terms of sums over the positions $\mathbf{r}_{i_\alpha}$ of all monomers in the system of type α as

$$\Delta\hat{\rho}_\alpha(1) = \hat{\rho}_\alpha(1) - \rho_\alpha(1) = \sum_{i_\alpha}\delta(1-\mathbf{r}_{i_\alpha}) - \langle\sum_{i_\alpha}\delta(1-\mathbf{r}_{i_\alpha})\rangle \tag{27}$$

The symbols $\langle\ \rangle$ in eqs 25–27 denote grand-canonical averages.[20]

Translational invariance of a homogeneous polymer melt of volume V and eqs 25 and 26 imply the Fourier transforms of eqs 21 and 22 as

$$\Gamma_3(\mathbf{q}_1,\mathbf{q}_2,\mathbf{q}_3) = -D_s(q_1)\,D_t(q_2)\,D_v(q_3)\,G_{stv}(\mathbf{q}_1,\mathbf{q}_2,\mathbf{q}_3) \tag{28}$$

and

$$\begin{aligned}\Gamma_4(\mathbf{q}_1,\mathbf{q}_2,\mathbf{q}_3,\mathbf{q}_4) = \\ D_s(q_1)\,D_t(q_2)\,D_v(q_3)\,D_w(q_4)\,\gamma_{stvw}(\mathbf{q}_1,\mathbf{q}_2,\mathbf{q}_3,\mathbf{q}_4)\end{aligned} \tag{29}$$

with

$$D_\alpha(q) = S_{A\alpha}^{-1}(q) - S_{B\alpha}^{-1}(q) \tag{30}$$

and

$$\begin{aligned}\gamma_{stvw}(\mathbf{q}_1,\mathbf{q}_2,\mathbf{q}_3,\mathbf{q}_4) = &-G_{stvw}(\mathbf{q}_1,\mathbf{q}_2,\mathbf{q}_3,\mathbf{q}_4) + \\ &V^{-1}[G_{stm}(\mathbf{q}_1,\mathbf{q}_2,-\mathbf{q}')\,S_{mn}^{-1}(q')\,G_{nvw}(\mathbf{q}',\mathbf{q}_3,\mathbf{q}_4) + \\ &G_{svm}(\mathbf{q}_1,\mathbf{q}_3,-\mathbf{q}')\,S_{mn}^{-1}(q')\,G_{ntw}(\mathbf{q}',\mathbf{q}_2,\mathbf{q}_4) + \\ &G_{swn}(\mathbf{q}_1,\mathbf{q}_4,\mathbf{q}')\,S_{mn}^{-1}(q')\,G_{mvt}(-\mathbf{q}',\mathbf{q}_3,\mathbf{q}_2)]\end{aligned} \tag{31}$$

The wave vectors $\mathbf{q}'$ are chosen to maintain translational invariance in each term of eq 31. So, for example, $G_{stv}(\mathbf{q}_1,\mathbf{q}_2,\mathbf{q}')$ has $\mathbf{q}' = -\mathbf{q}_1 - \mathbf{q}_2$. Also, Γ_3 vanishes unless $\mathbf{q}_1 + \mathbf{q}_2 + \mathbf{q}_3 = 0$ as does Γ_4 except when $\mathbf{q}_1 + \mathbf{q}_2 + \mathbf{q}_3 + \mathbf{q}_4 = 0$. Note that the form of eqs 28 and 31 does not place any constraints on the correlation functions used in actual calculations. Rather, these results follow as a consequence of an application of the incompressibility condition to well-known results from the theory of liquids. The RPA vertex functions are obtained upon replacing the correlation functions $G_{stv}(\mathbf{q}_1,\mathbf{q}_2,\mathbf{q}_3)$ and $G_{stvw}(\mathbf{q}_1,\mathbf{q}_2,\mathbf{q}_3,\mathbf{q}_4)$ and the inverse structure factors with their ideal, Gaussian-chain analogues.

III. A Numerical Study of the Fourth-Order RPA

Having derived the second-, third-, and fourth-order vertex functions of a binary system in the previous section, we now proceed to study the segregation of lamellar, block-copolymer mesophases. The functional

$$\Omega_V[\{\rho_i(\mathbf{R})\}] = F[\{\rho_i(\mathbf{R})\}] - \sum_\alpha\int d1\;\rho_\alpha(1)\;\phi_\alpha(1) \tag{32}$$

is minimized[20,26] by the equilibrium densities. We model $F[\{\rho_i(\mathbf{R})\}]$ using the prescription discussed in the previous section as

$$F[\{\rho_i(\mathbf{R})\}] = F_G[\{\rho_i(\mathbf{R})\}] + F_{local}[\{\rho_i(\mathbf{R})\}] \tag{33}$$

Now consider only those density variations that respect the incompressibility condition (i.e., eq 9). Then near a homogeneous state having densities ρ_A^0 and ρ_B^0 and total density ρ, $F[\{\rho_i(\mathbf{R})\}]$ has the functional expansion

$$\begin{aligned}F[\{\rho_i(\mathbf{R})\}] = F[\{\rho_i^0\}] + \frac{\rho^2}{2}\int d1\int d2\;\Gamma_2(1,2)\;\psi(1)\;\psi(2) + \\ \frac{\rho^3}{6}\int d1\int d2\int d3\;\Gamma_3(1,2,3)\;\psi(1)\;\psi(2)\;\psi(3) + \\ \frac{\rho^4}{24}\int d1\int d2\int d3\int d4\;\Gamma_4(1,2,3,4)\;\psi(1)\;\psi(2)\;\psi(3)\;\psi(4)\end{aligned} \tag{34}$$

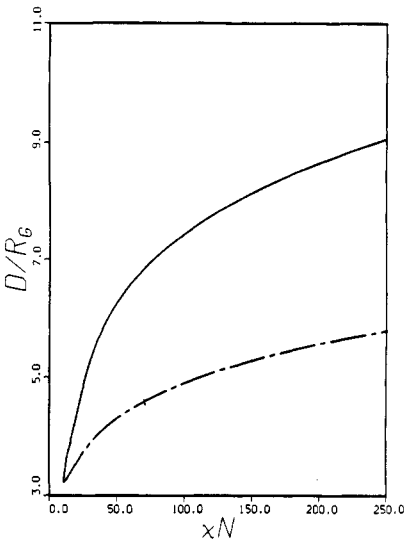

Figure 1. Domain spacing as a function of χN below the phase transition. The solid curve is for the fourth-order calculations whereas the chain-dashed curve plots the results of the second-order ones.

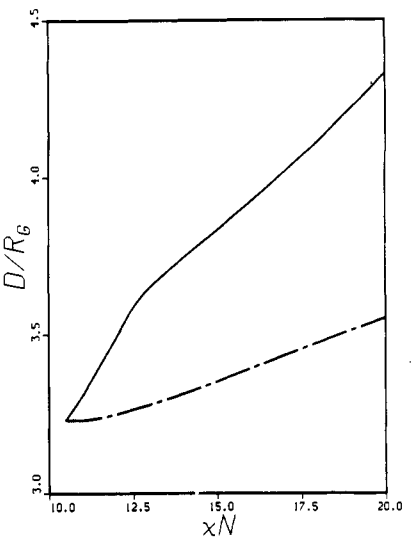

Figure 2. An enlarged view of the transition region of Figure 1. The legend for the curves is the same as in Figure 1.

where

$$\psi(1) = [\rho_A(1) - \rho_A^0]/\rho \tag{35}$$

Following Melekevitz and Muthukumar,[14,27] we consider a Gaussian-window function

$$\psi(z) = \sum_{i=-\infty}^{\infty} H(z - iD) \tag{36}$$

$$H(z) = \frac{1}{(2\sigma^2\pi)^{1/2}} \int_{z-fD/2}^{z+fD/2} dy\, e^{-y^2/(2\sigma^2)} \tag{37}$$

σ and D are variational parameters that we employ to approximately minimize Ω_V, and f denotes the fraction of A monomer in the copolymer chains. Since the overall monomer number density does not change (within the incompressibility approximation) upon cooling the melt through the microphase separation, it suffices to minimize $F[\{\rho_i(\mathbf{R})\}]$. In the limit that $\sigma \to 0$, $\psi(z)$ reduces to a square wave of periodicity D. It also resembles the cosine wave $\cos(2\pi z/D)$ for $\sigma/D \geq 0.3$.

In Figures 1–3, we present some results for the minimization of $F[\{\rho_i(\mathbf{R})\}]$ at $f = 0.5$. These calculations employ the RPA-approximate correlation functions for $\Gamma_2(q_1)$, $\Gamma_3(q_1,q_2)$, and $\Gamma_4(q_1,q_2,q_3)$. We convert the integrals appearing in $F[\{\rho_i(\mathbf{R})\}]$ to sums over the Fourier components of $\psi(z)$. These sums converge rapidly for the WSL calculations shown in Figure 2, but for the examples with the smallest values of σ (those at the largest χN's), they involve many Fourier components.

The natural length scale in the present problem is the radius of gyration R_G of an ideal, diblock chain. Note that R_G scales as $N^{1/2}$ [23,24] so if $D/R_G \propto N^{\nu'}$ over some range of χN values in Figures 1 and 2, $D \propto N^{\nu}$ with $\nu = \nu' + 1/2$. We observe that the domain spacing D grows more rapidly than $N^{1/2}$ immediately below the microphase separation χN, consistent with the observations of earlier research.[12,15,16] At fixed N, D increases upon cooling the melt below the transition temperature. This occurs even over the range of temperatures for which a single wave vector determines the morphology (i.e., the weak-segregation limit).

To better understand the behavior of the domain spacing in the WSL, consider $F[\{\rho_i(\mathbf{R})\}]$ when $f = 0.5$. The third-order vertex functions $\Gamma_3(q_1,q_2,q_3)$ vanish for this composition, and the present theory predicts that the microphase separation is second order and occurs near $\chi N = 10.495$. A single Fourier component

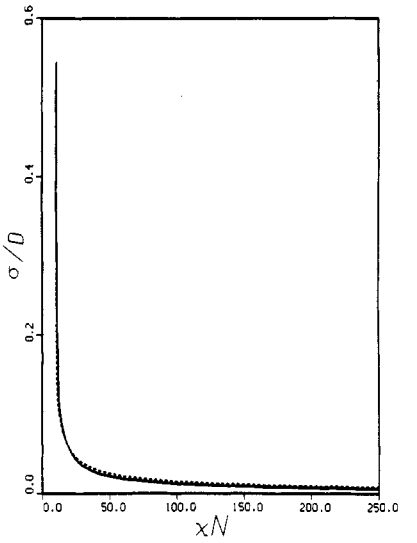

Figure 3. Interfacial width parameter σ below the phase transition: solid curve, fourth-order calculations; dotted curve, second-order calculations.

$$\psi(z) \approx \hat{\psi}(2\pi/D)\cos(2\pi z/D) \tag{38}$$

of periodicity D dominates and we can write

$$\Delta F[\{\rho_i(\mathbf{R})\}] \approx \rho^2\Gamma_2(q,-q)\psi_1^2 + \frac{\rho^4}{4}\Gamma_4(q,-q,q,-q)\psi_1^4 \tag{39}$$

where $q = 2\pi/D$, $\psi_1 = \hat{\psi}(q)$, $q = 2\pi/D$, and

$$\Delta F[\{\rho_i(\mathbf{R})\}] = F[\{\rho_i(\mathbf{R})\}] - F[\{\rho_i^0\}] \tag{40}$$

Minimizing eq 39 with respect to ψ_1 leads to

$$\Delta F[\{\rho_i(\mathbf{R})\}] \approx -\frac{\Gamma_2(q,-q)^2}{\Gamma_4(q,-q,q,-q)} \quad \text{(WSL)} \tag{41}$$

We then determine D by minimizing this result with respect to q. Reference 14 approximates $\Gamma_4(q,-q,q,-q)$ in eq 40 with $\Gamma_4(q^*,-q^*,q^*,-q^*)$, where q^* denotes the wave vector at the onset of the microphase separation. As Leibler[6] has pointed out, $\Gamma_2(q,-q)$ has a maximum at q^*. Thus, when Γ_4 = a constant, $q = q^*$ irrespective of χN as

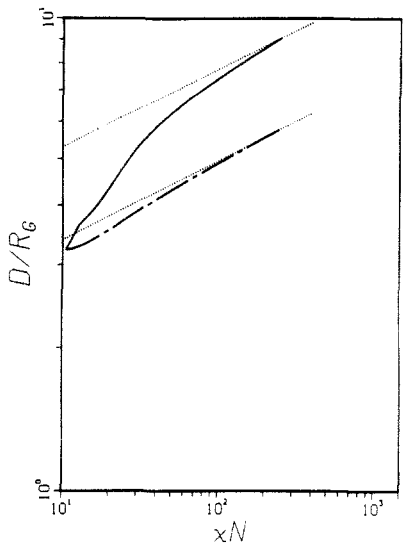

Figure 4. Log–log plot of the data of Figure 1. The solid curve is for the fourth-order calculations and the chain-dashed curve for the second-order ones. The dotted lines drawn adjacent to the curves have slopes of 1/6 as would a scaling relationship $D \propto N^{2/3}$ plotted on this graph.

long as the single-wave approximation (eq 38) applies. However, when we retain the full wave-vector dependence of $\Gamma_4(q,-q,q,-q)$, we find that q changes linearly with χN and fails to produce a simple scaling law of the sort $D \propto N^{\alpha}$. This follows from the fact that $\Gamma_4(q,-q,q,-q)$ does not have an extremum at q^* so that small changes in q may produce a lower value of $\Delta F[\{\rho_i(\mathbf{R})\}]$ than that obtained at q^*. Thus, as the polymer melt is cooled below $\chi N = 10.495$, the domains immediately begin to grow relative to their threshold value and σ decreases. σ decreases even upon approximating $\Gamma_4(q,-q,q,-q)$ with the constant $\Gamma_4(q^*,-q^*,q^*,-q^*)$ because

$$\psi_1 = \frac{1}{\pi}\exp(-\pi^{2\mathrm{Hexx}\sigma^2/D^2}) = \left[\frac{-2\Gamma_2(q^*,-q^*)}{\rho^2\Gamma_4(q^*,-q^*,q^*,-q^*)}\right]^{1/2} \quad \text{(WSL)} \tag{42}$$

in this case. Reducing the temperature makes $-\Gamma_2(q^*)$ larger, causing ψ_1 to grow. With D fixed, ψ_1 can only increase if σ decreases. From eq 42 we see that

$$\frac{\mathrm{d}(\sigma/D)^2}{\mathrm{d}(\chi N)} \propto -\frac{1}{\chi N - \chi^* N} \tag{43}$$

in the WSL with χ^* the Flory parameter at the onset of the microphase separation. Figure 3 illustrates the rapid decrease of σ predicted by this result. Note that the singularity in σ near the transition is a consequence of the continuous nature of the transition and obtains even when we include the proper q dependence of $\Gamma_4(q,-q,q,-q)$ in eq 42. At the critical point, $\sigma = \infty$ so that $\psi_1 = 0$. Upon cooling the melt sufficiently to observe a finite-amplitude density wave, σ is finite. At off-critical compositions, σ remains finite even at the transition.

Close to the transition, we observe a rapid increase of D/R_G with χN for the reasons already mentioned. D/R_G increases more slowly at large values of χN and starts to approach the 2/3 law. Figure 4 replots the results of Figure 1 on a log–log graph to show this. Note that the lower curve (which we have yet to discuss) has nearly reached the SSL $D \propto N^{2/3}$ limit for $\chi N > 100$. However, even at the largest values of χN considered in Figures 1 and 4, the apparent exponent of the upper curve is still about 0.71. [For comparison, we plot relations of the type $D/R_G \propto N^{1/6}$ near the curves on the graph to make the deviation of the data from the scaling relation obvious.] This, however, represents a significant decrease from its peak value of about 1 which occurs when $\chi N \approx 30$ and it appears that at very large χN, D should scale as $N^{2/3}$. Reference 15, which employs the scf technique to calculate $F_G[\{\rho_i(\mathbf{R})\}]$, quotes a value of $D/R_G = 5.96$ at $\chi N = 125$ whereas, for comparison, we find $D/R_G = 7.80$—about a 30% error. The difference in the results stems from the consistently too large scaling exponent between D and N in the present calculations.

In many studies of inhomogeneous systems and phase transitions, it proves helpful to separate from the rest of the free energy an ideal functional that derives from the properties of a noninteracting system[13,20,28] and can be evaluated to infinite order in the relevant density order parameters. This functional usually has the form of an entropy of mixing and, in the absence of external fields, favors a homogeneous distribution of the system's components. However, the connectivity of the block polymer chains makes it impossible to define an unambiguous, "ideal" free energy for block copolymers in an external field. The ideal free energy describes the response of the chain to an infinitely slowly varying external field. If the field acts on A and B monomers in the same way, we recover the ideal state used in ref 14. In the case of a blend or homopolymer solution, similar arguments lead to the Flory–Huggins entropy of mixing.[29] However, even when the fields do not vary appreciably over length scales comparable to the size of fully extended blocks, the presence of different fields for A and B monomers can result in profound segregation effects. We allow for these effects in the nonlocal parts of $F[\{\rho_i(\mathbf{R})\}]$. Thus, to account in a qualitative way for the possibility that an all-orders, ideal, free energy functional affects block-copolymer segregation, we propose the heuristic ideal functional

$$F_{\mathrm{mix}}[\psi(\mathbf{R})] = \frac{\rho}{N}\int \mathrm{d}1 \left\{f(1)\ln\left[\frac{f(1)}{f}\right] + [1-f(1)]\ln\left[\frac{1-f(1)}{1-f}\right]\right\} \tag{44}$$

with $f(1) = f + \psi(1)$. Equation 44 bears some resemblance to the ideal free energy of mixing different homopolymers.[23,24] A derivation of eq 44 based on a block copolymer in a slowly varying field[30] motivates this form but also illustrates that an unambiguous definition of F_{mix} does not exist. A slightly different choice of the "ideal state"[13] yields an F_{mix} without the $1/N$ prefactor in eq 44. Such a choice would lead to a separate dependence of the system properties on χ and N, which we do not pursue in the present analysis. [Note that the RPA form for the correlation functions leads to a dependence of the segregation properties on χN rather than on χ and N separately.] However, without the reduction achieved by the $1/N$ factor, the ideal terms become much more significant.

Rather than expanding F_{mix} to fourth order as we have done for $F[\{\rho_i(\mathbf{R})\}]$, we retain the all-orders form of eq 44. Adding and subtracting eq 44 to the intrinsic free energy functional, we have

$$F[\{\rho_i(\mathbf{R})\}] = F_{\mathrm{mix}}[\{\rho_i(\mathbf{R})\}] + \{F_G[\{\rho_i(\mathbf{R})\}] - F_{\mathrm{mix}}[\{\rho_i(\mathbf{R})\}]\} + \frac{\beta}{2}\sum_{\alpha\beta} u_{\alpha\beta}\int \mathrm{d}1\, \rho_\alpha(1)\,\rho_\beta(1) \tag{45}$$

Now expand the difference

$$F_G[\{\rho_i(\mathbf{R})\}] - F_{mix}[\{\rho_i(\mathbf{R})\}] + \frac{\beta}{2}\sum_{\alpha\beta} u_{\alpha\beta}\int d1\ \rho_\alpha(1)\ \rho_\beta(1)$$

to fourth-order in $\psi(1)$ for the incompressible case. This expansion is

$$F'_{RPA}[\psi(\mathbf{R})] = F_G[\psi(\mathbf{R})] - F_{mix}[\psi(\mathbf{R})] + \frac{\beta}{2}\sum_{\alpha\beta} u_{\alpha\beta}\int d1\ \rho_\alpha(1)\ \rho_\beta(1) =$$

$$F[\{\rho_i^0\}] + \frac{\rho^2}{2}\int d1\int d2\ \Gamma_2^m(1,2)\ \psi(1)\ \psi(2) +$$

$$\frac{\rho^3}{6}\int d1\int d2\int d3\ \Gamma_3^m(1,2,3)\ \psi(1)\ \psi(2)\ \psi(3) +$$

$$\frac{\rho^4}{24}\int d1\int d2\int d3\int d4\ \Gamma_4^m(1,2,3,4)\ \psi(1)\ \psi(2)\ \psi(3)\ \psi(4) \quad (46)$$

The coefficients in eq 46 are related to the ordinary RPA vertex functions by

$$\Gamma_2^m(1,2) = \Gamma_2(1,2) + \frac{\delta(1-2)}{\rho f(1-f)} \quad (47a)$$

$$\Gamma_3^m(1,2,3) = \Gamma_3(1,2,3) - \frac{\delta(1-2)\ \delta(1-3)(1-2f)}{\rho^2[f(1-f)]^2} \quad (47b)$$

and

$$\Gamma_4^m(1,2,3,4) = \Gamma_3(1,2,3) + \frac{2\delta(1-2)\ \delta(1-3)\ \delta(1-4)(1-3f+3f^2)}{\rho^3[f(1-f)]^3} \quad (47c)$$

Because it includes F_{mix}, eq 46 contains all orders of the Fourier components of $\psi(1)$ in contrast to eq 34, which only includes fourth- and lower-order combinations of the $\psi(q)$'s. The calculations with and without F_{mix} as described below show that the wave-vector dependence of the third- and fourth-order vertex functions play a much more important role in determining the segregation than does the assumed form for this "entropy-of-mixing-like" contribution. This contrasts the situation encountered in theories of the interfaces of blends[31] and homopolymer solutions,[29,32] where the entropy of mixing can lead to a pronounced asymmetry of the relevant interface. We expect that any reasonable *local* approximation for F_{mix} proportional to $1/N$ would yield similar results. Alternative formulations of block-copolymer[13,33] or polyatomic molecular[34] thermodynamics which treat bonds as perturbations would lead to ideal contributions not proportional to $1/N$. These could have a profound effect on the segregation process.

We have repeated our calculations for the segregation of the lamellar phase using eqs 46–47 in place of eq 34. On the scale of Figures 1–4, the results are indistinguishable from those of the fourth-order calculations that do not include F_{mix}. Comparing the calculations in detail, we do find that including the ideal term predicts a slightly slower initial development of segregation than the theory based on eq 34. Considered by itself, F_{mix} favors a homogeneous distribution of monomeric components and softens somewhat the rate of decrease of σ and increase of D with increasing χN. However, the inclusion of F_{mix} also alters the part of the free energy functional that we approximate by the fourth-order expansion. Thus, to fourth order, eq 34 and eqs 45–47 are equivalent and the fifth- and higher-order parts of F_{mix} actually cause the initial slowing of the domain sharpening and growth. Once the segregation has become pronounced, F_{mix} saturates to a SSL value of $(\rho V/N)$ ln 2 and plays very little role in determining the morphology. The effect of F_{mix} is quite small (less than 10%) and not discernible in Figures 1–4.

Finally, we repeat the fourth-order calculations summarized by the solid curves in Figures 1–4 by using only the second-order expansion of F'_{RPA}. In other words, we set $\Gamma_3^m(1,2,3)$, $\Gamma_4^m(1,2,3,4)$, etc. in eq 46 to zero but retain F_{mix}. These calculations illustrate the role of the fourth-order terms in determining the segregation of the supercooled melt. Compared to the fourth-order calculations, the second-order ones predict that the domain spacing and the segregation (as parametrized by σ) increase more slowly with χN. The initial increase in D with χN clearly scales as $N^{1/2}$ as we measure D in units of R_G, the radius of gyration of ideal chains, which itself scales as $N^{1/2}$. In the SSL, the calculations approach the $D \propto N^{2/3}$ law much more rapidly than the fourth-order ones presented in Figure 1. Because we neglect the third- and higher-order terms in the expansion of F'_{RPA}, the coefficients of the generic term

$$\hat{\psi}(q_1)\ \hat{\psi}(q_2)\ \hat{\psi}(q_3)\ \hat{\psi}(q_4) \quad (48)$$

are independent of $\mathbf{q}_1$, $\mathbf{q}_2$, $\mathbf{q}_3$, and $\mathbf{q}_4$, and our results resemble those of ref 14. For the chain-dashed curve in Figure 4, D scales as $D \propto N^{2/3}$ by the time χN reaches 100. Furthermore, we see that D/R_G is almost constant over the range $10.495 < \chi N < 11.0$ in Figure 2. However, the more accurate RPA functional which includes the fourth-order vertex function does not predict this result.

We mention in passing that neglecting the third- and fourth-order vertex functions without the presence of the ideal term (or an alternative, all-orders functional) generally produces an unsatisfactory free energy functional. The incompressibility constraint and/or the variational form for $\psi(z)$ can force stability, but the resulting minimization of

$$\Delta F[\{\rho_i(\mathbf{R})\}] \approx \frac{\rho^2}{2}\sum_q \Gamma_2(q,-q)\ \hat{\psi}^2(q) \quad (49)$$

leads to pathological segregation effects. The global minimum of eq 49 occurs when the Fourier coefficients $\hat{\psi}(q)$ assume their maximum absolute values for $\Gamma_2(q,-q) < 0$ but vanish when $\Gamma_2(q,-q) > 0$. Thus, even in the WSL, a single, Fourier mode leads to large overall density variations when one employs eq 49, and σ does not obey eq 43.

IV. Discussion

The numerical calculations described in the previous section all predict the same basic sequence of events, namely, that a second-order phase transition occurs near $\chi N = 10.495$ for a symmetric diblock copolymer followed by domain growth and sharpening. However, only the approximation that neglects the fourth-order coefficient in the expansion of the nonideal free energy about the homogeneous state predicts that $D \propto N^{1/2}$ for slight undercoolings, and only this approximation agrees with those experimental studies[2] which observe the $N^{1/2}$ scaling relation in the WSL. On the other hand, another group of experiments[35] suggest that the WSL exponent should have a value close to $\nu = 0.8$. Given that practically any theory that one might invent has a nonstationary fourth-order coefficient, it would seem rather remarkable if real block-copolymer systems do indeed obey the $N^{1/2}$ scaling.

Olvera de la Cruz[12] and Tang and Freed[16] reach essentially the same conclusions using the fourth-order expansion. One could argue that these analyses neglect fluctuations which might somehow stabilize an $N^{1/2}$ law. However, Olvera de la Cruz's calculations,[16] which employ the Hartree approximation,[36] apparently eliminate this possibility.

The contrasting approximation schemes we employ reveal a profound sensitivity of the results for D at moderate and large χN to the order of the truncation of the functional expansion of the nonideal free energy. The results exhibit less dependence on the inclusion of an all-orders, entropy-of-mixing-like quantity in the approximation for $F_G[\{\rho_i(\mathbf{R})\}]$. Thus, we find that the calculations which employ the correct fourth-order RPA vertex function predict that the limit $D \propto N^{2/3}$ is approached more slowly than in the second-order theory. This results from the rapid initial increase of D with χN in the WSL. At larger degrees of segregation, the domain spacing's dependence on N and χ tends to relax to the SSL predictions, but it has to relax much more than in the second-order case, where D initially scales as $N^{1/2}$. Questions which we cannot completely address then naturally arise about the significance of the higher-order terms neglected in the functional expansion. Perhaps the next-order terms in the vertex function expansion would restore a more rapid approach to the SSL observed in the scf calculations and the second-order theory, but that possibility seems counterintuitive. The fourth-order theory clearly shows, however, that the SSL occurs only beyond $\chi N = 100$—an observation corroborated by other[14,15] theoretical calculations. This contrasts recent experimental observations in which Anastasiadis et al.[3] measure an apparent scaling relation of the form $N^{0.65}$ in almost symmetric samples of polystyrene–poly(methyl methacrylate) copolymers. As mentioned in ref 14, the highest-molecular-weight samples of these authors only have $\chi N = 105$. This makes it highly unlikely that these authors have truly measured the domain scaling in the SSL. Of course, our results depend on a number of physical and mathematical simplifications. The most significant of these include the use of Gaussian statistics to approximate the nonlocal contributions to the free energy, the application of the random-mixing approximation to account for the temperature dependence of $F[\{\rho_i(\mathbf{R})\}]$, and, in the present calculations, the truncation of the functional expansion of the nonlocal parts of the free energy.

Experimental studies[3] of diblock copolymers provide evidence that the width of the interface separating domains does not depend on temperature ($1/\chi$) or the polymerization number. We define the interfacial width a_I as

$$a_I = \frac{\pi[(f(z))_{max} - f]}{|(df/dz)_{f(z)=f}|} \tag{50}$$

The definition of $f(z)$—eqs 36 and 37, and $f(z) = \psi(z) + f$, and its symmetry—$f(z) = 1/2$ at $z = D/4$ and $(f(z))_{max} = f(0)$ leads to the general results

$$|(df/dz)_{f(z)=f}| = \frac{4}{D}\sum_{n=1}^{\infty} e^{-2\pi^2(2n-1)^2(\sigma/D)^2} \tag{51a}$$

and

$$(f(z))_{max} = f + \frac{2}{\pi}\sum_{n=1}^{\infty}\frac{(-1)^{n+1}}{(2n-1)} e^{-2\pi^2(2n-1)^2(\sigma/D)^2} \tag{51b}$$

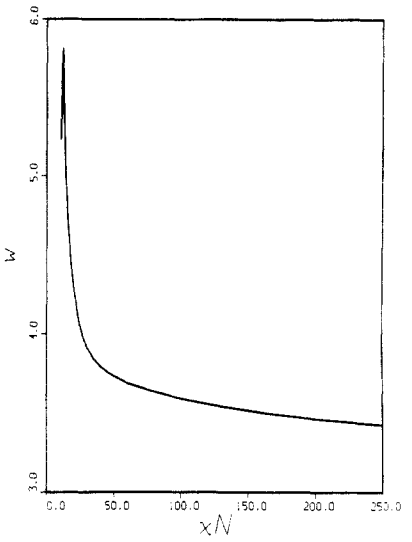

Figure 5. The quantity w, related to the interfacial width a_I through $w = a_I(\chi N)^{1/2}/R_G$ (eq 50 defines a_I), in the segregated melt for the fourth-order calculations.

for $f = 1/2$. However, in the WSL, these reduce to

$$|(df/dz)_{f(z)=f}| = \frac{4}{D}e^{-2\pi^2(\sigma/D)^2} \quad \text{(WSL)} \tag{52a}$$

and

$$(f(z))_{max} = f + \frac{2}{\pi}e^{-2\pi^2(\sigma/D)^2} \quad \text{(WSL)} \tag{52b}$$

For strongly segregated domains, we find

$$|(df/dz)_{f(z)=f}| = \frac{1}{D[2(\sigma/D)^2\pi]^{1/2}}(1 - e^{-1/[8(\sigma/D)^2]}) \quad \text{(SSL)} \tag{53a}$$

and

$$(f(z))_{max} = 1 \quad \text{(SSL)} \tag{53b}$$

Equations 53a,b follow most directly from the real-space definition of $\psi(z)$ (eq 36) and the observation that only the $i = 0$ term contributes significantly in the limit of small σ/D. The WSL results, eqs 52a,b, are obtained from the Fourier expansions of $\psi(z)$ (or $f(z)$) upon retaining only the longest-wavelength term. The numerator of eq 50 facilitates calculations of the effective interfacial widths in the WSL and is defined so that in the WSL, $a_I = D/2$. Put another way, the interface encompasses the entire domain in the WSL. Slight variations[3,15,37] of this definition appear elsewhere in the literature. However, we are not presently interested in absolute numbers but in the constancy or lack of constancy of the interfacial width.

We express D in units of R_G—the ideal-chain polymer radius of gyration—so that a_I has units R_G also. In the SSL, we expect[5,15] that the quantity $w = a_I(\chi N)^{1/2}/R_G$ approaches π. In Figures 5 and 6, we plot w for the fourth-order calculations (both types, with and without F_{mix}, yield almost identical results). Clearly, a_I varies considerably. Near the transition (see Figure 6), $a_I = D/2$ and w rises with χN because D also increases. w subsequently shrinks as segregation effects begin to dominate at larger χN. For the largest values of χN considered, w varies slowly with temperature and/or N. However, the RPA does not predict an a_I independent of χN. In particular, w—and thus a_I—is particularly sensitive to χN in the intermediate- and weak-segregation ranges. Again, it appears that w becomes independent of χN as this quantity approaches ∞. However, numerical problems with the convergence of the fourth-order sums over vertex functions make calculations

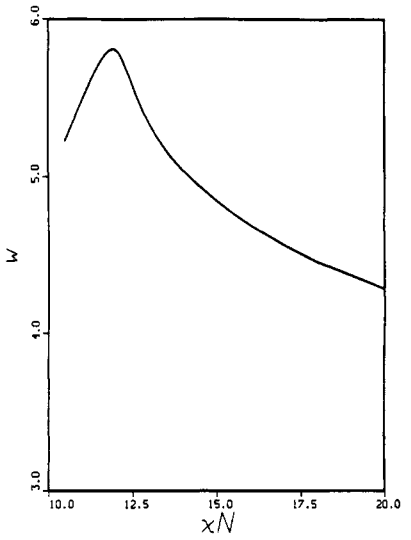

Figure 6. An enlarged view of the region near the phase transition for the data of Figure 5.

at values of χN larger than about 300 infeasible. Figures 5 and 6 do establish that the fourth-order RPA approaches the SSL, as measured by the constancy of w, quite slowly.

We conclude this section by briefly discussing some fundamental connections between the vertex-function-based calculations, the scf approach, and the functional integral, field-theory formulation of block-copolymer phase transitions. In the scf theory, one generates the Gaussian part of $F[\{\rho_i(\mathbf{R})\}]$ (i.e., the first part of eq 1) by solving a modified diffusion equation.[5] Until recently,[15] published, exact, numerical solutions to this problem did not exist. This observation provides a testament to the difficulties encountered when trying to solve the scf equations—essentially integral–partial-differential equations. However, when solved numerically in this fashion, the scf approach yields the exact solution to the model free energy given by eq 1. In general, little is known about the stability of the technique when modeling $F_{\text{local}}[\{\rho_i(\mathbf{R})\}]$ with a more realistic and hence more complicated form in place of eq 2. The vertex-function expansion can be derived directly from Edwards' Hamiltonian[38] as in ref 9a using functional integrals. This methodology allows for systematic improvements incorporating fluctuations[10,12] into the analysis. Alternatively, the vertex-functions can be regarded as functional derivatives of a model free energy like that in eqs 1 and 2. In that case, the free energy implies the Hamiltonian,[20] and the exact minimization of the grand potential (eq 32) represents the exact summation of the partition function corresponding to this Hamiltonian. However, the Hamiltonian does not necessarily closely resemble an intuitive molecular rendering of a diblock copolymer. The second-order cumulant techniques used in refs 9a, 18, and 19 yield the same free energy as eq 1. However, at higher order, this technique produces a different expression for $F[\{\rho_i(\mathbf{R})\}]$. One should, therefore, not surmise that the free energy functional (eq 1) of the RPA and scf formalisms maps onto the Edwards Hamiltonian even though all three approaches to block-copolymer thermodynamics lead, at varying degrees of approximation, to the same free energy functional.

V. Summary and Conclusions

The RPA clearly follows from a division of the intrinsic free energy functional into a local, random-mixing approximation for monomer–monomer interactions and a functional for inhomogeneous Gaussian chains. Similar demonstrations of the equivalence of simple theories of blends and homopolymers to density-functional formalisms have already appeared in the polymer literature.[29,31] Imposing an incompressibility constraint on the correlation functions derived from this functional leads to the traditional RPA, but one can also obtain compressible analogues. More significantly, the decomposition of $F[\{\rho_i(\mathbf{R})\}]$ into Gaussian and local parts suggests new ways to approximate the two pieces of the free energy functional.

For instance, we can imagine perturbation expansions, about the noninteracting Gaussian state, which lead to more accurate expressions for the interaction part of the free energy functional. This would naturally introduce a somewhat inelegant and rather complicated dependence of the free energy on monomer–monomer interaction parameters, but it could also lead to important modifications in the shape of the theoretical structure factor. In the RPA theory, the position of the structure factor's peak (or, alternatively, the position of the second vertex function's minimum) does not depend on the temperature. This contradicts the results of both experiments[35a,c] and simulations[39] which show that at temperatures above the block-copolymer microphase separation, the blocks stretch in order to minimize monomer–monomer contacts, resulting in a more general shape of the partial monomer–monomer structure factors. Including chain stretching in the model would result in new theoretical predictions for the behavior of the domain sizes and interfacial widths. With regards to the noninteracting, entropic part of $F[\{\rho_i(\mathbf{R})\}]$, studies of the freezing transitions of atomic systems[20,41] have benefited from all-orders free energy functionals which avoid truncations like the fourth-order approximation used in this paper. Future theories could be constructed to satisfy sum rules on the free energy functional[20] or expand the free energy about local values of the density as in ref 29. It may also be useful to construct a variational theory in terms of the chain-end distribution function used in scf theories.[5,15] All of these techniques yield all-orders functionals which, though approximate, might prove capable of better describing the SSL. These and other methodologies for developing density functionals of highly inhomogeneous block copolymer fluids will be the subjects of future publications. Developing approximations for $F_G[\{\rho_i(\mathbf{R})\}]$ that can accurately account for the relative stability of the ordered phases, facilitate fast numerical calculations, and qualitatively describe the segregation of monomers within the different types of domains remains a difficult and largely unaddressed problem.

The present calculations employ more conventional approximations obtained by expanding $F[\{\rho_i(\mathbf{R})\}]$ to fourth order about a homogeneous melt. Although such finite-order treatments can lead to quantitative discrepancies in the SSL, a comparison of the fourth-order expansion to the scf methodology reveals some of the strengths and weaknesses of the expansion methodology.

The fourth-order RPA density functional provides a reasonably good *qualitative* description of the lamellar microphase separation despite its quantitative failings. In fact, the calculations described in the present article exhibit no profound qualitative defects. We can compare the fourth-order results to those of the scf theory because the two formalisms employ the same continuous-Gaussian-chain model to approximate correlations in a polymer melt. Thus, at infinite order, the vertex-function expansion of eq 1 yields the same results as the scf, modified-diffusion technology. Although the predicted values of D deter-

mined variationally from the fourth-order theory are systematically too large, the calculation of a_I—the interfacial width—agrees remarkably well with that determined by the full-blown scf calculations.[15]

One could always argue that the successes and/or weaknesses of the present theory may stem from the trial function used to describe the segregation process. Experience with density-functional applications to other systems (see, for example, ref 29 and references cited therein) suggests that the basic formalism is, however, quite insensitive to the assumed form of the density provided that form provides a qualitatively reasonable picture of the true profiles. Clearly, the symmetric Gaussian-window trial function will not duplicate certain details of the exact profiles as determined[15] numerically, but at this stage, we can only remark that the differences between the present results and those calculated from the scf equations[15] are qualitatively quite minor. More concrete observations about the sensitivity of the fourth-order expansion's predictions must await additional calculations performed with alternative trial functions.

Compared to the calculations described in ref 14 which ignore the wave-vector dependence of the third and fourth vertex functions, the present theory provides a much more accurate description of the WSL. We expect that the wave-vector dependence of the fourth-order terms should have a similar impact on theories of surface-imposed ordering[42] in near-critical block copolymer melts or in descriptions of other block-copolymer mesophases. We plan to extend our calculations of the lamellar morphology to body-centered cubic, hexagonal, and even bicontinuous double-diamond morphologies in future work.

Acknowledgment. This research is supported, in part, by grants from the Robert A. Welch Foundation (A-1175) and the donors of the Petroleum Research Fund (Grant 25613-AC7B), administered by the American Chemical Society.

References and Notes

(1) Noshay, A.; McGrath, J. E. *Block Copolymers*; Academic Press: New York, 1989. *Block Copolymers*; Aggarwal, S. L., Ed.; Plenum: New York, 1970. *Developments in Block Copolymers—I*; Goodman, I., Ed.; Applied Science: New York, 1982. *Processing, Structure, and Properties of Block Copolymers*; Folker, M. J., Ed.; Elsevier: New York, 1985.
(2) Green, P. F.; Russell, T. P.; Jerome, R.; Granville, M. *Macromolecules* **1988**, *21*, 3266.
(3) Anastasiadis, S. H.; Russell, T. P.; Satija, S. K.; Majkrzak, C. F. *J. Chem. Phys.* **1990**, *92*, 5677.
(4) Bates, F. S. *Science* **1991**, *251*, 898.
(5) Helfand, E. *Macromolecules* **1975**, *8*, 552. Helfand, E.; Wasserman, Z. *Ibid.* **1976**, *9*, 879; *Polym. Eng. Sci.* **1977**, *17*, 582.
(6) Leibler, L. *Macromolecules* **1980**, *13*, 1602.
(7) Hong, K. M.; Noolandi, J. *Macromolecules* **1983**, *16*, 1083.
(8) Semenov, A. N. *Zh. Eksp. Teor. Fiz.* **1985**, *88*, 1242 [*Sov. Phys. JETP* **1985**, *61*, 733].
(9) (a) Ohta, T.; Kawasaki, K. *Macromolecules* **1986**, *19*, 2621. (b) The 2/3 power law has been derived also by Di Marzio, E. A.; Guttman, C. M.; Hoffman, J. D. *Macromolecules* **1980**, *13*, 1194; and Di Marzio, E. A. *Ibid.* **1988**, *21*, 2262.
(10) Fredrickson, G. H.; Helfand, E. *J. Chem. Phys.* **1987**, *87*, 697.
(11) Mayes, A. M.; Olvera de la Cruz, M. *J. Chem. Phys.* **1989**, *91*, 7228.
(12) Olvera de la Cruz, M. *Phys. Rev. Lett.* **1991**, *67*, 85.
(13) McMullen, W. E.; Freed, K. F. *J. Chem. Phys.* **1990**, *93*, 9130.
(14) Melenkevitz, J.; Muthukumar, M. *Macromolecules* **1991**, *24*, 4199.
(15) Shull, K. R. *Macromolecules* **1992**, *25*, 2122. See also: Vavasour, J. D.; Whitmore, M. D. *Ibid.* Self-Consistent, Mean-Field Theory of the Microphases of Diblock Copolymers. *Ibid.*, in press.
(16) Tang, H.; Freed, K. F. *J. Chem. Phys.* **1991**, *95*, 3012.
(17) Schweizer, K. S.; Curro, J. G. *Phys. Rev. Lett.* **1988**, *60*, 809.
(18) Brereton, M. G.; Vilgis, T. A. *J. Phys. (Paris)* **1989**, *50*, 245.
(19) McMullen, W. E.; Freed, K. F. *Macromolecules* **1990**, *23*, 255.
(20) Evans, R. *Adv. Phys.* **1979**, *28*, 143. Evans, R. *Microscopic Theories of Simple Fluids and Their Interfaces*; Charvolin, J., Joanny, J. F., Zinn-Justin, J., Eds.; Elsevier: Les Houches, 1989.
(21) In fact, a monodisperse system of block copolymers has but a single chemical potential which couples to the overall number density of chains or monomers. Independent fluctuations of the number densities of different types of monomers are impossible. For homopolymer mixtures (blends), each polymeric component contributes one unique chemical potential to the thermodynamics and the different monomer densities can fluctuate independently. The formal consequences of the stoichiometry are discussed at length in ref 16.
(22) Hansen, J. P.; McDonald, I. R. *Theory of Simple Liquids*; Academic: New York, 1976.
(23) de Gennes, P.-G. *Scaling Concepts in Polymer Physics*; Cornell University Press: Ithaca, NY, 1979.
(24) Flory, P. J. *Principles of Polymer Chemistry*; Cornell University Press: Ithaca, NY, 1953.
(25) Reference 6, Appendix A.
(26) Hohenberg, P.; Kohn, W. *Phys. Rev. B* **1964**, *136*, 864. Mermin, N. D. *Phys. Rev. A* **1965**, *137*, 1441.
(27) Note that eqs 36 and 37 differ slightly from the variational function used in ref 5. In the present article we shift $\psi(z)$ to make it an even function of z. This simplifies somewhat the numerical calculations because half the Fourier coefficients vanish.
(28) McMullen, W. E.; Freed, K. F. *J. Chem. Phys.* **1990**, *92*, 1413.
(29) McMullen, W. E. *J. Chem. Phys.* **1991**, *95*, 8507. McMullen, W. E. *Physics of Polymer Surfaces and Interfaces*; Sanchez, I. C., Ed.; Butterworths: Stoneham, MA, 1992.
(30) McMullen, W. E.; unpublished notes.
(31) Tang, H.; Freed, K. F. *J. Chem. Phys.* **1991**, *94*, 1572, 6307.
(32) Szleifer, I.; Widom, B. *J. Chem. Phys.* **1989**, *90*, 7524.
(33) Freed, K. F.; Bawendi, M. G. *J. Phys. Chem.* **1989**, *93*, 2194 and references cited therein.
(34) Wertheim, M. S. *J. Stat. Phys.* **1986**, *35*, 19, 35; **1986**, *42*, 459, 477.
(35) (a) Hadziioannou, G.; Skoulios, A. *Macromolecules* **1982**, *15*, 258. (b) Owens, J. N.; Gancarz, I. S.; Koberstein, J. T.; Russell, T. P. *Ibid.* **1989**, *22*, 3380. (c) Almdahl, K.; Rosedale, J. H.; Bates, F.; Wignall, G. D.; Fredrickson, G. H. *Phys. Rev. Lett.* **1990**, *65*, 1112.
(36) Amit, D. J.; Zanetti, M. *J. Stat. Phys.* **1973**, *9*, 1. Brazovskii, S. A. *Zh. Eksp. Teor. Fiz.* **1975**, *68*, 175 [*Sov. Phys. JETP* **1975**, *41*, 85].
(37) Meier, D. J. *Thermoplastic Elastomers—Research and Development*; Legge, N., Holden, G., Schroeder, H., Eds.; Hanser: München, Germany, 1988. Wu, S. *Polymer Interface and Adhesion*; Marcel Dekker: New York, 1982. Fernandez, M. L.; Higgens, J. S.; Penfold, J.; Ward, R. C.; Shackelton, C.; Walsh, D. J. *Polymer* **1988**, *29*, 1923.
(38) Edwards, S. F. *Proc. Phys. Soc. London* **1965**, *85*, 613.
(39) Fried, H.; Binder, K. *J. Chem. Phys.* **1991**, *94*, 8349; *Europhys. Lett.* **1991**, *16*, 237.
(40) Tang, H.; Freed, K. F. *J. Chem. Phys.* **1992**, *96*, 8621.
(41) See, e.g.: Haymet, A. D. J. *Annu. Rev. Phys. Chem.* **1987**, *38*, 89.
(42) Fredrickson, G. H. *Macromolecules* **1987**, *20*, 2535.